Geomagnetic disturbances and their relationship to Interplanetary shock parameters

S. Jurac, J. C. Kasper, J. D. Richardson, and A. J. Lazarus
Massachusetts Institute of Technology, Cambridge, Massachusetts, USA

Received 4 September 2001; revised 15 February 2002; accepted 19 February 2002; published 28 May 2002.

[1] We identify 107 fast, forward-propagating interplanetary shocks observed by the Wind spacecraft from 1995–2000 to examine the influence of shock parameters on geomagnetic disturbances following the shock arrival at Earth. We find that the angle between the shock front normal and the interplanetary magnetic field (IMF) direction might play a useful role in forecasting the severity of geomagnetic storms occurring within 48 hours from the shock passage. Quasi-perpendicular shocks, i.e. those nearly orthogonal to the IMF direction, constrain IMF components in the plane parallel to the shock front, making it more likely to produce southward IMF. We demonstrate that, regardless of the shock driver, about 40% of forward IP shocks result in intense magnetic storms when the shock normal is almost perpendicular to the IMF, compared to about 10–15% of shocks with normals not perpendicular to the IMF direction. *INDEX TERMS:* 2139 Interplanetary Physics: Interplanetary shocks; 2164 Interplanetary Physics: Solar wind plasma; 2134 Interplanetary Physics: Interplanetary magnetic fields; 2109 Interplanetary Physics: Discontinuities

1. Introduction

[2] Forward interplanetary (IP) shocks are known precursors of the arrival of larger solar structures leading to geomagnetic disturbances. They are followed by regions of compressed magnetic field and enhanced plasma densities, which cause geomagnetic disturbances via interaction with Earth's magnetic field. Two principal mechanisms which drive IP shocks are: a) the interaction of solar wind streams with different speeds (CIRs), and b) transient phenomena such as Coronal Mass Ejections (CMEs) propagating through the interplanetary medium. CIRs are characterized by a fluctuating magnetic field and produce only weak or moderate storms [*Tsurutani et al.*, 1995].

[3] Intense magnetic storms (Dst < -100) tend to develop when a southward-pointing IMF ($B_z < -10$ nT) lasts more than three hours [*Gonzalez and Tsurtani*, 1987]. CMEs are followed by looplike, outwardly-propagating structures [e.g. *Wu et al.*, 2001; *Wood et al.*, 1999] which are ejected into interplanetary space. When an interplanetary CME (ICME) moves faster than the solar wind speed, a shock forms on its leading edge, compressing the pre-existing IMF. This mechanism sometimes generates intense, long-lasting, southward fields (B_S) which result in magnetic storms. A strong association has been observed previously between ICMEs and IP shocks [*Watari and Watanabe*, 1998; *Tsurutani et al.*, 1995; *Lindsay et al.*, 1994]; between IP shocks and magnetic clouds [*Lepping et al.*, 2001; *Luhman*, 1997]; and between IP shocks and resulting geomagnetic disturbances [*Gonzalez et al.*, 1999; *Tsurutani et al.*, 1992; *Gonzalez and Tsurutani*, 1998]. Recently, *Webb et al.* [2000] found that all of the six observed halo CMEs that were Earthward directed were associated with shocks and magnetic clouds, eventually resulting in magnetic storms 3–5 days later. Besides magnetic clouds, a particular class of CMEs which exhibit a smooth rotation in magnetic field direction, magnetic storms are also caused by complex ejecta. These complex ejecta, possibly produced by the interaction of two or more CMEs [*Burlaga et al.*, 2001], are characterized by highly disorganized IMF directions.

[4] It is possible to observe Earthward-directed CMEs and current efforts are focused on infering their general magnetic topology in real time from space-based solar observatories such as SOHO and Yohkoh. Resulting forward IP shocks can be observed from near-Earth spacecraft upon their arrival at L1, which gives approximately an hour lead time before they reach Earth. However, predicting the strength and longevity of B_S is still full of uncertainties, because the IMF is frequently highly fluctuating. *Chen et al.* [1997] showed that for particularly well-defined magnetic structures, such as flux ropes and magnetic clouds, B_S could be predicted up to approximately 10 hours in advance. For such structures, the smooth rotation of the IMF observed at an L1 monitor allows extrapolation of B_S to later times when the event reaches Earth. In this paper we search for properties of IP shocks which foreshadow geomagnetic disturbances in the following 48 hours. We find a relationship which is not clearly related to the shock driver.

2. Method

[5] The IP shocks are analyzed using plasma data from the wind Faraday Cup Solar Wind Experiment (SWE) and magnetic field data from the Magnetic Field Instrument (MFI), covering the period from Wind launch in late 1994 to the end of 2000. The magnetic field data were obtained at 3-second time resolution. A plasma spectrum measurement is initiated every 90 seconds and the time to complete a spectrum varied from 60 to 90 seconds depending on the instrument mode.

[6] The immediate 20 minutes of data on either side of the shock (excluding measurements within the shock itself) are used to characterize the upstream and downstream plasma parameters. Sharp increases in bulk speed, IMF magnitude, and density of at least 3%, 20% and 30% respectively, were required downstream compared to the upstream values. Every shock candidate was examined by eye, and if an unrelated event contaminated pre- or post-shock intervals, the period was shortened to exclude that event. At least 10 valid measured data points on either side of the shock were required or the shock was discarded. Shock parameters were determined using five methods: magnetic coplanarity, velocity coplanarity, and three mixed methods, [e.g. *Schwartz*, 1998; *Russell et al.*, 1983; *Russell et al.*, 2000]. In total, 132 fast forward IP shocks were examined and 107 selected, since no clear determination of the front normal direction was possible for 25, mostly weaker shocks.

[7] To check the shock parameter determination, we examined the shock arrival times for nine IP shocks also observed by the ACE spacecraft when Wind and ACE were separated by less than 25 R_E in the perpendicular direction ($\sqrt{Y^2 + Z^2}$ in GSE). At this proximity, both spacecraft were likely to observe the same front normal and the five methods were compared. The expected arrival time of the shock at one spacecraft was then calculated by

0094-8276/02/2001GL014034$05.00

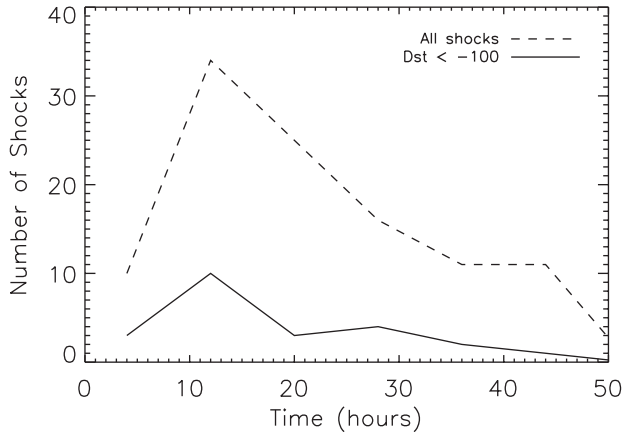

Figure 1. Delay time between shock arrival and Dst minimum, binned in 8 hr intervals. The dashed line represents all shocks while solid line shows shocks followed by large geomagnetic storms (Dst < −100).

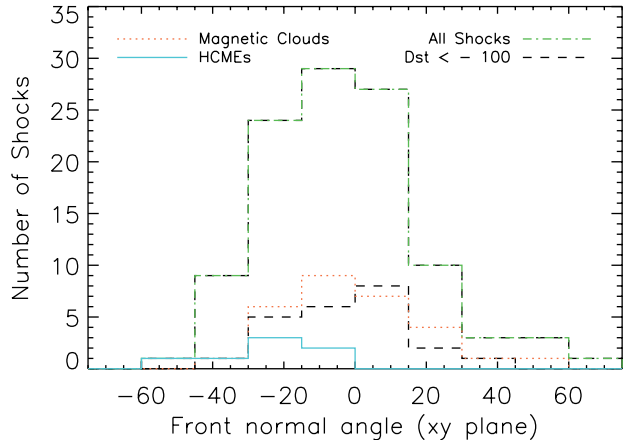

Figure 3. Distribution of shock normal angles (measured clockwise from −X in GSE) in X-Y plane for all shocks (dash-dot), shocks with Dst < −100 (dash), shocks associated with magnetic clouds (dot), and with halo CMEs (solid).

propagating the shock front (assumed to be planar) with the shock speed in the front-normal direction to the other spacecraft. This predicted arrival time was then compared to the measured shock arrival time, enabling independent assessment of the quality of the shock normals determined using the different methods. *Russell et al.* [2000] analyzed one large shock and found that the magnetic coplanarity method produced a more accurate result than the other methods; they attributed that result to the much higher time resolution of MFI data used. Surprisingly, for the larger sample used here, magnetic coplanarity did not lead to a superior determination of the shock normal direction. Inherently, the magnetic coplanarity (MC) and velocity coplanarity (VC) methods fail for strictly perpendicular or parallel shocks, and additionally MC is sensitive to short-term fluctuations in IMF direction. Predictions of the shock arrival time determined by the three mixed methods was superior to those based on the MC or VC methods. The difference in results between the three mixed methods were superior and their average was used to determine the direction of the shock front normals.

[8] Θ_{Bn}, sometimes referred to as the 'obliquity angle', represents the angle between the direction of the shock front normal and the upstream magnetic field: parallel IP shocks propagate parallel to the IMF, perpendicular shocks propagate perpendicular to the IMF, while oblique shocks lie in between these two cases. For nine shocks observed by both Wind and ACE, the average deviation between the front normals was 3° (11° for θ_{Bn}), in general agreement with deviations between different spacecraft found by *Russell et al.* [2000]. The front normal directions determined here are on the average 2–3 times more accurate than those in *Jurac and Richardson* [2001], who used the best correlation between IMF parameters at different spacecraft to determine the front normal directions. Our θ_{Bn} values differ on the average by ±9° from those of *Berdichevsky et al.* [2000] who used the Rankine-Hugoniot method. These uncertainties, as shown later, are unlikely to affect our conclusions.

[9] Using the predicted arrival time of the shock front at Earth, we determined the minimum Dst value in the following 48 hour interval. If we chose a time period longer than 48 hours, multiple shocks often corresponded to the same Dst minimum and a direct causal relation between an individual shock and the corresponding Dst minimum was less clear. The same two-day, post-shock period was previously used by *Gonzalez and Tsurtani* [1987]. In three cases, where ambiguity existed because two comparable shocks were observed within a day, both shocks were assigned the same Dst minimum value.

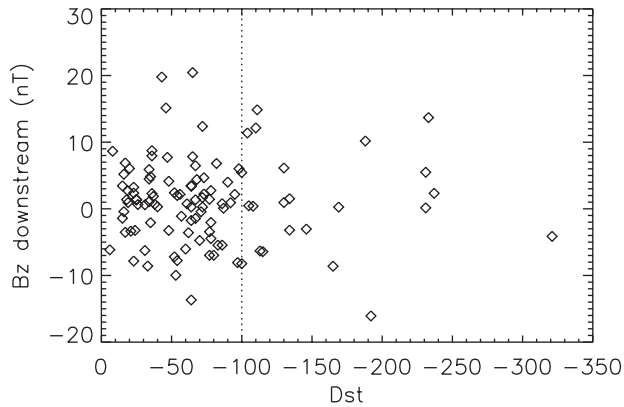

Figure 2. Dst vs. Bz values measured immediately downstream from the shock. B_S (B_z < 0) does not correlate with the geoeffectiveness of the magnetic storm.

3. Results

[10] The delay time between shock passage and the Dst minima, binned in eight-hour intervals, is shown in Figure 1. Most of the storms reached minimum Dst within a day after shock passage and about a third during the following day. Out of 23 shocks preceding intense magnetic storms (Dst < −100), 17 Dst minima occurred in the first 24 hours and the remainder during the following day. The IMF direction and, consequently, the B_S magnitude, frequently showed a substantial variation on a time scale shorter than a day.

[11] Figure 2 shows B_z values measured downstream from the shock and no correlation with the Dst index is evident. B_z following the shock arrival is oriented northward half of the time even in the cases of the intense magnetic storms (Dst < −100). Thus, although the shock is a precursor to the compressed, southward IMF which eventually produces magnetic storms, the IMF measured at the shock passage does not correlate with the storm intensity. Figure 3 shows the distribution of the ecliptic plane components of front normal directions, F_n, for all events (dash-dot line) and for those with Dst < −100 (dashed line). The front normals are measured from the −X direction in the GSE coordinate system, with positive angles in the +Y direction. The mean value and the standard deviation are $F_n = -3.4 \pm 21.9°$, consistent with the $-5 \pm 23°$ found by *Berdichevsky et al.* [2000] at 1 AU and

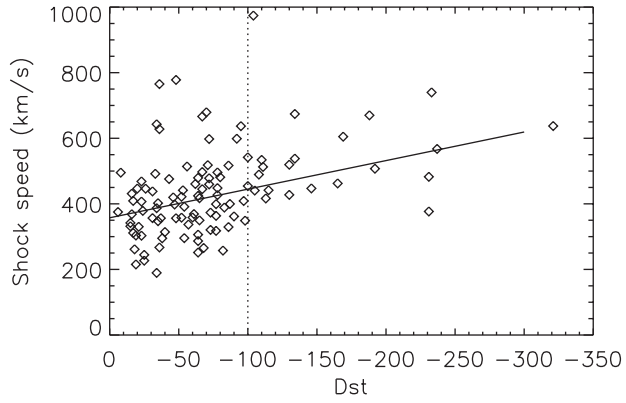

Figure 4. Dst index vs. shock speed; the solid line shows a linear fit through data (Correlation coefficient = 0.41).

the −3.8° found by *Lindsay et al.* [1994] as the mean front angle at 0.72 AU. An equivalent distribution is seen for Dst < −100, with no preferential direction observed for geoeffective shocks (F_n = −2.0 ± 18°). A similar distribution was observed in the GSE X-Z plane (not shown). In Figure 3 we also show front normal distributions for shocks followed by a magnetic cloud (dotted line) and for shocks preceded by halo CMEs (solid).

[12] Unlike the front normal direction and B_z at the shock front, the shock speed shows some correlation with the storm intensity

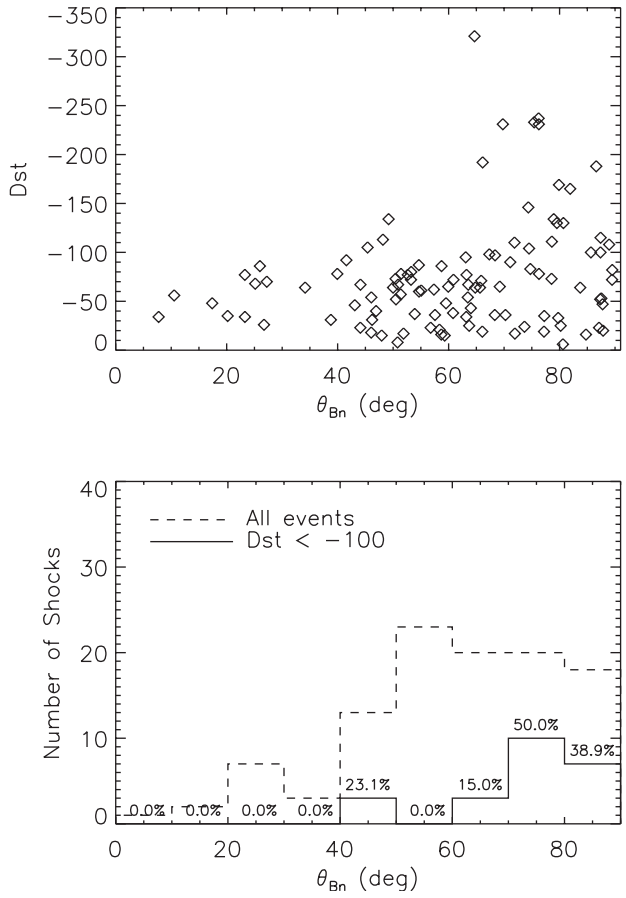

Figure 5. (a) Shock geoeffectivness vs. Θ_{Bn}. (b) Number of shocks observed for Θ_{Bn} in 10° bins for all events (dashed) and Dst < −100 (solid). The percentages represent the proportion of geoeffective shocks (Dst < −100).

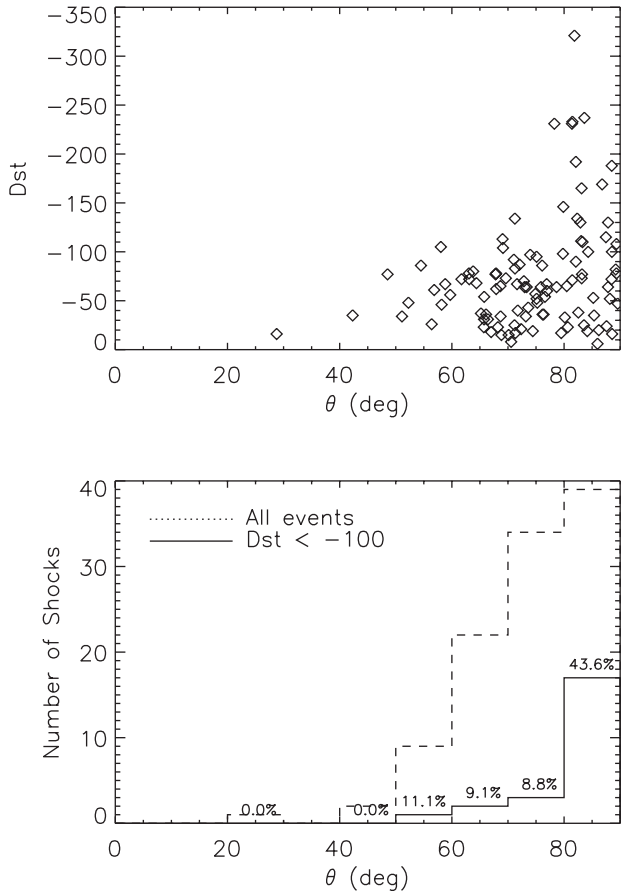

Figure 6. Same as Fig. 6 for Θ, which is the angle between the downstream IMF and the shock front normal direction.

(Figure 4). A weak relationship between the solar wind plasma velocity and storm intensity was found earlier [e.g. *Tsurutani et al.*, 1987]. Since many of the fastest shocks (>600 km/s) do not produce geoeffective storms, the shock speed, as found earlier for plasma velocity, has little predictive value.

[13] In contrast with the results above, the angles that the shock front normal makes with IMF upstream and downstream (i.e. in front of and behind the shock ramp), seems to be a much better indicator of the future geoeffectivness. Figures 5a and 6a show the angle between the shock normal and the upstream IMF (Θ_{Bn}) and downstream IMF (Θ) plotted vs. Dst for all analyzed shocks. Shocks with larger Θ_{Bn} values, i.e. those propagating "more perpendicular" to the IMF direction, generally produce larger magnetic storms. The ten largest storms observed all occurred for θ_{Bn} values larger than 60° (Figure 5a). The histogram given in Figures 5b and 6b shows the number of all observed shocks and those with Dst < −100 for each 10° bin in θ_{Bn} and θ. The shocks with Θ_{Bn} between 70–90° result in the intense storms 38–50% of the time, i.e. they are more than twice as likely to result in a magnetic storm than shocks with lower Θ_{Bn} values.

[14] As expected, the compressed, post-shock field tends to be more orthogonal to the shock front normal. The resulting distribution (Figure 6a) is squeezed toward larger angles, and only a few shocks producing intense magnetic storms (Dst < −100) have Θ < 80°. Since the uncertainty in the angle between the IMF and front normal is about 10°, 83% of the geoeffective shocks (19 out of 23) have a propagation direction orthogonal to the downstream IMF. The peak in Θ_{Bn} at 50° observed in Figure 5b (dashed line) is a simple consequence of the undisturbed IMF field geometry, i.e., the average IMF being along

the Parker spiral and the typical shock front normal oriented close to −X direction (Figure 3).

[15] The angle between shock normal and the downstream IMF, Θ, (Figure 6) provides an even greater ability to differentiate between the geoeffective and non-geoeffective shocks than does Θ_{Bn} (Figure 5). It appears that the association found is largely due to those events that carry substantial shock-compressed B_S fields. Shocks with front normals orthogonal to the downstream IMF are more than four times as likely to result in intense storms than non-orthogonal ones ($\Theta < 80°$). When the IMF is orthogonal to the shock propagation direction, shock compression of the pre-existing IMF enhances the field strength. Although the southward IMF component might not be present immediately behind the shock front, we found a substantial likelihood (~40%) that in the 48 hours following the shock sufficiently strong B_s will appear, inducing a geomagnetic storm. The downstream IMF is more constrained to the plane parallel to the shock front (predominantly the Y-Z plane), increasing the likelihood that with later evolution a strong southward B_z will occur. For shocks with front normals not perpendicular to the IMF, less field compression occurs and the probability for sufficiently strong B_S following a shock is reduced. Finally, our finding does not appear to be a consequence of most geoeffective events being more aligned with the radially outward (−X) direction. As seen in Figure 3, no preferential radial direction is observed for more geoeffective events (solid line), compared to all events (dashed). Also, no preferential alignment of Θ nor Θ_{Bn} vs. front normal direction was found (not shown). The front normal direction, Θ and Θ_{Bn} were examined vs. shock driver (CME, magnetic cloud, CIR) and no statistically significant difference was found. The front normals for seven shocks associated with halo CME were all found in the X-Y quadrant orthogonal to the Parker spiral (Figure 3).

4. Summary

[16] According to *Wu and Dryer* [1996] the initial IMF turning direction at 1 AU for CME related events could be inferred at the shock's arrival. *Chen et al.* [1997] showed that for well-defined magnetic structures such as flux ropes and magnetic clouds, B_S could be predicted up to approximately 10 hours in advance. For such structures, the smooth rotation of the IMF allows extrapolation to later times, making it possible to predict southward turning and estimate the B_S component which causes geoeffective storms. In contrast, the complex ejecta are characterized by highly variable and, essentially, unpredictable IMF direction. In this paper we demonstrate that, when a well-defined magnetic structure is not evident which is the case most of the time, the angle between shock front normal and IMF can be used to enhance the predictive abilities of spacecraft monitors. We find that there is about a 40% chance for a forward IP shock to be followed by an intense magnetic storm when its front normal is perpendicular to the IMF. Those 'perpendicular' shocks are 2 – 4 times more likely to result in an intense storm than shocks that do not propagate orthogonal to the IMF direction. Although the uncertainty for such predictions remains larger then by extrapolating IMF rotation at future time as in *Chen et al.* [1997], since most of the magnetic structures following the shocks are not 'well-behaved', this method may be applied more generally, regardless of a specific IMF configuration.

[17] **Acknowledgments.** This work was supported by NSF Space Weather program under grants ATM-9613935 and ATM-9819699. The authors wish to thank David Webb for providing a list of halo CMEs and referees for helpful comments.

References

Berdichevsky, D. B., et al., Interplanetary fast shocks and associated drivers observed through the 23rd solar minimum by Wind over its first 2.5 years, *J. Geophys. Res.*, *105*, 27,289–27,314, 2000.

Burlaga, L. F. et al., Fast ejecta during the ascending phase of solar cycle 23: ACE observations, 1998–1999, *J. Geophys. Res.*, submitted, 2001.

Chen, J., P. J. Cargill, and P. J. Palmadesso, Predicting solar wind structures and their geoeffectiveness, *J. Geophys. Res.*, *102*, 14,701–14,720, 1997.

Gonzalez, W. D., and B. T. Tsurtani, Criteria of interplanetary parameters causing intense magnetic storms (Dst < −100 nt), *Planet. Space Sci.*, *35*, 1101–1109, 1987.

Gonzalez, W. D., and B. T. Tsurutani, The interplanetary causes of magnetic storms: A review., in *Magnetic Storms*, edited by B. T. Tsurutani, W. D. Gonzalez, Y. Kamide, and J. K. Arballo, AGU monograph 98, Washington, D.C., 1998.

Gonzalez, W. D., B. T. Tsurtani, and C. de Gonzalez, Interplanetary origin of geomagnetic storms, *Space Science Reviews*, *88*, 529–562, 1999.

Jurac, S., and J. D. Richardson, The dependence of plasma and magnetic field correlations in the solar wind on geomagnetic activity, *J. Geophys. Res.*, *106*, 29,207–29,915, 2001.

Lepping, R. P. et al., Upstream shocks and interplanetary magnetic cloud speed and expansion: Sun, Wind and Earth observations, *Adv. Space Res.*, in press, 2001.

Lindsay, G. M., C. T. Russell, and J. G. Luhmann, On the sources of interplanetary shocks at 0.72 AU, *J. Geophys. Res.*, *99*, 11–17, 1994.

Luhman, J., CMEs and space weather, in *Coronal Mass Ejections*, edited by N. Crooker, J. A. Joselyn, and J. Feynman, AGU Monograph 99, Washington, D.C., 1997.

Russell, C. T., Multiple spacecraft observations of interplanetary shocks: Four spacecraft determination of shock normals, *J. Geophys. Res.*, *88*, 4739–4748, 1983.

Russell, C. T., The interplanetary shock of September 24, 1998: Arrival at Earth, *J. Geophys. Res.*, *105*, 25,143–25,154, 2000.

Schwartz, S. J., Shock and discontinuity normals, mach numbers, and related parameters, in *Analysis Methods for Multi-Spacecraft Data*, edited by G. Paschmann and P. W. Daly, ISSI Scientific Report, ESA Publications Division, Netherlands, 1998.

Tsurutani, B. T., et al., Interplanetary origin of geomagnetic activity in the declining phase of the solar cycle, *J. Geophys. Res.*, *100*, 717–733, 1995.

Tsurutani, B. T., et al., Great magnetic storms, *Geophys. Res. Lett.*, *19*, 73–76, 1992.

Watari, S., and T. Watanabe, The solar drivers of geomagnetic disturbances during solar minimum, *Geophys. Res. Lett.*, *25*, 2489–2492, 1998.

Webb, D. F., et al., Relationship of halo coronal mass ejections, magnetic clouds, and magnetic storms, *J. Geophys. Res.*, *105*, 7491–7508, 2000.

Wood, B. E., et al., Comparison of two coronal mass ejections observed by EIT and LASCO with a model of an erupting magnetic flux rope, *Astrophys. J.*, *512*, 484–495, 1999.

Wu, C.-C., and M. Dryer, Predicting the initial Bz polarity's change at 1 AU caused by shocks that precede Coronal Mass Ejections, *Geophys. Res. Lett.*, *23*, 1709–1712, 1996.

Wu, S. T., M. D. Andrews, and S. P. Plunkett, Numerical Magnetohydrodynamics (MHD) modeling of Coronal Mass Ejections (CMEs), *Space Sci. Rev.*, *95*, 191–213, 2001.

S. Jurac, J. C. Kasper, A. J. Lazarus, and J. D. Richardson, Massachusetts Institute of Technology, Center for Space Research, M.I.T. 37-662, 77 Massachusetts Avenue, Cambridge, MA 02139, USA. (jurac@space.mit.edu; jck@space.mit.edu; ajl@space.mit.edu; jdr@space.mit.edu)